Industrial Engineering Journal
ISSN: 0970-2555
Volume : 53, Issue 6, No.4, June : 2024

COMPUTATIONAL ANALYSIS OF HALL AND ION SLIP EFFECTS ON THE MHD FLOW OF NANO FLUID ALONG AN INCLINED PLATE EMBEDDED IN A POROUS MEDIUM

P.Raveendra Nath, Lecturer in Mathematics, Sri Krishnadevaraya University College of Engineering and Technology, S.K.University, Anantapur - 515 003, A.P., India.
E-mail id:ravindrasku@gmail.com
Dinesh Kumar S. T. , Associate Professor, Department of Mathematics, Government Science college Chitradurga, Karnataka

ABSTRACT
The radiative MHD flow of an incompressible viscous electrically conducting non-Newtonian vertical porous surface has been considered. Under the influence of slip velocity in a rotating frame, it takes Hall and ion slip impacts into account.The Laplace transformation technique is employed on the non-dimensional governing equations to ensure closed-form analytical solutions. The graphical representations scrutinize the effects of physical parameters on the significant flow characteristics. The present study is of immediate interest in next-generation solar film collectors, heat-exchanger technology,material processing exploiting vertical and inclined surfaces, geothermal energy storage,and all those processes which are greatly affected by a heat-enhancement concept.

Key words: Nanofluid' Porous medium, Heat Transfer, CFD

Introduction
A nanofluid is a fluid containing nanometer-sized particles, called nanoparticles. These fluids are engineered colloidal suspensions of nanoparticles in a base fluid. The nanoparticles used in nanofluids are typically made of metals (Al, Cu), oxides (Al2O3, CuO, TiO2, SiO2), carbides (SiC), nitrides (AlN, SiN), or nonmetals (graphite, carbon nanotubes), and the base fluid is usually a conductive fluid, such as water or ethylene glycol. Other base fluids are oil and other lubricants, bio-fluids and polymer solutions. Nanoparticles are particles that are between 1 and 100 nm in diameter. Nanofluids commonly contain up to a 5% volume fraction of nanoparticles to see effective properties over the properties of the base fluid.Nanofluids have novel properties that make them potentially useful in many applications in heat transfer, including microelectronics, fuel cells, pharmaceutical processes, and hybrid-powered engines. They exhibit enhanced thermal conductivity and convective heat transfer coefficient compared to the base fluid.

Choi [1] to indicate engineered colloids composed of nanoparticles dispersed in a base fluid. The characteristic feature of nanofluids is thermal conductivity enhancement, a phenomenon observed by Masuda et al. [2]. A comprehensive survey of convective transport in nanofluids was made by Buongiorno [3] based at MIT, who considered two-phase non-homogenous model seven slip mechanisms that can produce a relative velocity between the nanoparticles and the base fluid: inertia, Brownian diffusion, thermophoresis, diffusiophoresis, Magnus effect, fluid drainage, and gravity. Of all of these mechanisms, only Brownian diffusion and thermophoresis were found to be important. Buongiorno's analysis [3] that a non-dimensional analysis of the equations implied that energy transfer by nanoparticle dispersion is negligible, and cannot explain the abnormal heat transfer coefficient increases. He further suggested that the boundary layer has different properties due to the effect of temperature and thermophoresis. The viscosity may be decreasing in the boundary layer,which would lead to heat transfer enhancement. An excellent assessment of nanofluid physics and developments has beenprovided by Das et al. [4] and Eastman et al. [5]. Buongiorno and Hu [6] observed that, although convective heat transferenhancement has been suggested to be due to the dispersion of the suspended nanoparticles, this effect is too small toexplain the observed enhancement. They further

assert that turbulence is not affected by the presence of the nanoparticles,so this cannot explain the observed enhancement.

Important studies in this regard have been madeby Bejan and Khair [7], Lai and Kulacki [8], and Murthy and Singh [9]. Coupled heat and mass transfer by mixedconvection in a Darcian fluid-saturated porous medium has been analysed by Lai [10]. More complex multiphysical thermalconvection flows in porous media have also been addressed. Bég et al. [11] further investigated magnetohydrodynamicfluid–particle suspension thermal convection in porous media. Bhargava et al. [12] studied transient chemically reactingmagneto-convective heat and mass transfer in porous media. Cheng [13] analysed the problem of combined free and forced(mixed) convection about inclined surfaces (or wedges) in a saturated porous medium on the basis of boundary layerapproximations. Chamkha [14] also investigated the natural convection from an inclined plate embedded in a variableporosity porous medium due to solar radiation.

The recent developments in technology require an innovative revolution in heat transfer.The research on nanofluids has been amplified fast. According to reports nanofluids are advantageous heat transport fluids for engineering and manufacturing applications. The heat transport development of nanofluids is principally reliant on the heat conductivity of nanoparticles, particles' volume concentration and mass flow discharges. Under steady particles' volume concentration and flow discharges, the heat transport development only on the heat conductivity of the nanoparticles.

An exhaustive and narrative review on heat transport investigation of predictable and hybrid nanofluids by the non-Newtonian fluid model was determined by Jamshed et al.[15] and Ellahi [16]. Aman et al. [17] exhibited the sodium alginate-based hybrid nanofluids (Copper-Alumina) flow in vertical ducts. Usman et al. [18] discussed the nonlinear thermal radiation and time-dependent heat conductivity due to rotating flow alumina-H2O hybrid nanofluids past a stretching sheet with a magnetic field and buoyancy force.Despite the complications of producing non-Newtonian fluids, applied mathematicians and engineers are engaged in non-Newtonian fluid mechanics. Because the flow and heat transport features of those fluids are significant to numerous and miscellaneous systems in bio-technology, pharmaceutical and chemical engineering, etc. Non-Newtonian modelling has a nonlinear relationship with the stress and rate of strain. The mechanical features of non-Newtonian fluids, and hear thin or shear thickness, usual stress difference, and visco-elastic reaction, may not be portrayed through the conservative theories; hence, an innovative and effectual prediction is required.Applications of extended, modified auxiliary equation mapping method for high-order dispersive extended nonlinear Schrödinger equation in nonlinear optics were discussed by Seadawy and Cheemaa [19]. Rizvi et al. [20] investigated the Biswas–Arshed model in birefringent fibers for chirp-free solitons with the aid of the sub-ordinary differential equations method. Seadawy and Cheemaa [21] investigated the propagation of nonlinear complex waves for the coupled nonlinear Schrödinger Equations in two core optical fibers. Seadawy et al. [22] explored the system of equations for the ion sound and Langmuir waves. Rizvi et al. [23] investigated the lump soliton solution for geophysical Korteweg–de Vries equation with the help of the Hirota bilinear method. Krishna [24] investigated the radiation absorption, chemical reaction, Hall and ion slip impacts on MHD free convection flow past a semi-infinite moving porous surface. The effects of Hall and ion slip on the radiative MHD rotating flow of viscous Jeffrey fluid over an infinite vertical flat porous surface by the ramped wall velocity and temperature were explored by Krishna [25].

Mathematical formulation of the problem

We assumed an unsteady MHD rotating flow of an incompressible electrically conducting viscous H_2O and ethylene glycol mixture (by volume ratios of 60 and 40) base Casson hybrid nanofluid($Ag - TiO_2/H_2O$) over an infinite rapidly accelerated vertical surface taking Hall and ion slip effects into account.

The consequence of rotating in the z-direction gives a transverse body strength to the flow. This in turn produces transversal velocity gradients (i.e. cross flow), and the flow becomes two-

dimensional. The flow of fluid under contemplation is subject to a steady uniform transverse magnetic field B_0 corresponding to the z-direction. The strength of the induced magnetic field due to fluid movement is assumed to be insignificant in contrast to the applied magnetic field. The consequence of polarization of fluid is disregarded due to the deficiency of applied electrical field.

$$\tau = \left(\mu_b + \frac{p_y}{\sqrt{2\pi}}\right) 2e_{ij,}\pi > \pi_c; \left(\mu_b + \frac{p_y}{\sqrt{2\pi_c}}\right) 2e_{ij,}\pi < \pi_c \quad (2.1)$$

whereπ is the product of the component of deformation rate through itself, namely, $\pi = e_{ij}e_{ij}, e_{ij}$ is the $(i,j)^{\text{th}}$ component of the rate of deformation and π_c is the significant estimation of π based on the non-Newtonian model. If $\pi < \pi_c$, the fundamental rheological equations of Casson fluid reduce as

$$\tau_{ij} = \mu_b \left(1 + \frac{1}{\beta}\right) 2e_{ij} \quad (2.2)$$

where $\beta = \mu_b \frac{\sqrt{2\pi}}{p_y}$. When $\beta \to \infty$, the non-Newtonian behavior of the fluid disappears, and the fluid performs similarly to a Newtonian fluid.

$$\begin{aligned} \rho_{hnf}\left(\frac{\partial q}{\partial t} + (q.\nabla)q + 2\Omega \times q\right) =& -\nabla p + \mu_{hnf}\left(1 + \frac{1}{\beta}\right)\nabla^2 q + (J \times B) \\ & - \frac{\mu_{hnf}}{K^*}\left(1 + \frac{1}{\beta}\right) q + g(\rho\beta_T)_{hnf}(T - T_\infty) \\ & + g(\rho\beta_C)_{hnf}(C - C_\infty) \end{aligned} \quad (2.3)$$

The component forms of Equation (2.3) when the pressure term is neglected

$$\begin{aligned} \frac{\partial u}{\partial t} - 2\Omega v =& v_{hnf}\left(1 + \frac{1}{\beta}\right)\frac{\partial^2 u}{\partial z^2} + \frac{B_0 J_y}{\rho_{hnf}} - \frac{v_{hnf}}{K^*}\left(1 + \frac{1}{\beta}\right) u \\ & + g(\beta_T)_{hnf}(T - T_\infty) + g(\beta_C)_{hnf}(C - C_\infty) \\ \frac{\partial v}{\partial t} + 2\Omega u =& v_{hnf}\left(1 + \frac{1}{\beta}\right)\frac{\partial^2 v}{\partial z^2} - \frac{B_0 J_X}{\rho_{hnf}} - \frac{v_{hnf}}{K^*}\left(1 + \frac{1}{\beta}\right) v \end{aligned} \quad (2.4)$$

The electron and atom collisions are assumed to be highly elevated; consequently, the Hall and ion slip impacts may not be deserted. For this reason, the Hall and ion slip consequences increase to the velocity in the y-direction.

$$J = \sigma(E + V \times B) - \frac{\omega_e \tau_e}{B_0}(J \times B) + \frac{\omega_e \tau_e \beta_i}{B_0^2}((J \times B) \times B)\Big) \quad (2.5)$$

Additionally, it is assumed that $\omega_e\tau_e \sim O(1)$and $\omega_i\tau_i << 1$, in Equation (2.5), the electron pressure gradient and thermo-electric effects are abandoned, i.e. the electric field $E = 0$ under these assumptions, Equation (2.5) is condensed to be

$$\begin{aligned} (1 + \beta_i\beta_e)J_x + \beta_e J_y &= \sigma B_0 V \\ (1 + \beta_i\beta_e)J_y - \beta_e J_x &= -\sigma B_0 u \end{aligned} \quad (2.6)$$

On solving Equations (2.6) we obtain

$$\begin{aligned} J_x &= \sigma B_0(\alpha_2 u + \alpha_1 v) \\ J_y &= -\sigma B_0(\alpha_2 v - \alpha_1 u) \end{aligned} \quad (2.7)$$

where$\alpha_1 = \frac{1+\beta_e\beta_i}{(1+\beta_e\beta_i)^2+\beta_e^2}$ and $\alpha_2 = \frac{\beta_e}{(1+\beta_e\beta_i)^2+\beta_e^2}$ Substituting Equations (2.7) in (2.5) and (2.4) accordingly, the equation of continuity, the momentum equation, energy and concentration equations are acquired.

Industrial Engineering Journal
ISSN: 0970-2555
Volume : 53, Issue 6, No.4, June : 2024

$$\frac{\partial u}{\partial x}+\frac{\partial v}{\partial y}=0$$

$$\begin{aligned}\frac{\partial u}{\partial t}-2\Omega v &= v_{hnf}\left(1+\frac{1}{\beta}\right)\frac{\partial^2 u}{\partial z^2}+\frac{\sigma_{hnf}B_0^2(\alpha_2 v-\alpha_1 u)}{\rho_{hnf}}-\frac{v_{hnf}}{K^*}\left(1+\frac{1}{\beta}\right)u\\ &\quad +g(\beta_T)_{hnf}(T-T_\infty)+g(\beta_C)_{hnf}(C-C_\infty)\\ \frac{\partial v}{\partial t}+2\Omega u &= v_{hnf}\left(1+\frac{1}{\beta}\right)\frac{\partial^2 v}{\partial z^2}-\frac{\sigma_{hnf}B_0^2(\alpha_2 u+\alpha_1 v)}{\rho_{hnf}}-\frac{v_{hnf}}{K^*}\left(1+\frac{1}{\beta}\right)v\end{aligned} \tag{2.8}$$

$$\left(\rho C_p\right)_{hnf}\frac{\partial T}{\partial t}=k_{hnf}\frac{\partial^2 T}{\partial z^2}-Q_0(T-T_\infty)$$

$$\frac{\partial C}{\partial t}=D_{hnf}\frac{\partial^2 C}{\partial z^2}-Kr^*(C-C_\infty)$$

The initial and boundary conditions for the flow past the electrically non-conducting plate with slip velocity are

$$\begin{aligned}&u=v=0, T=T_\infty, C=C_\infty, t\le 0, z>0\\ &u=u_0e^{t/t_0}+\lambda_0\left(1+\frac{1}{\beta}\right)\frac{\partial u}{\partial z}, v=\lambda_0\left(1+\frac{1}{\beta}\right)\frac{\partial v}{\partial z}\\ &T=\begin{cases}T_\infty+(T_w-T_\infty)(t/t_0), & \text{if } 0<t\le t_0\\ T_w & \text{if } t>t_0\end{cases}\\ &C=C_\infty+(C_w-C_\infty)(t/t_0)\\ &u\to 0, v\to 0, T\to T_\infty, C\to C_\infty, t>0, \text{as } z\to\infty\end{aligned} \tag{2.9}$$

Here $\lambda_0(\ge 0)$ is the slip coefficient and negative quantities of λ_0 did not keep in touch with physical cases

The effective properties of hybrid nanofluids are established by hybrids theory and phenomenon amendments.

$$\begin{aligned}\rho_{hnf}&=(1-\phi_2)\left[(1-\phi_1)_{\rho f}+\phi_1\rho_{s_1}\right]+\phi_2\rho_{s_2}, \mu_{hnf}=\frac{\mu_f}{(1-\phi_1)^{2.5}(1-\phi_2)^{2.5}},\\ \sigma_{hnf}&=\sigma_{bf}\left[\sigma_{s_2}(1+2\phi_2)+2\sigma_{bf}(1-\phi_2)\sigma_{s_2}(1-\phi_2)+\sigma_{bf}(2+\phi_2)\right],\\ \sigma_{bf}&=\sigma_f\left[\sigma_{s_1}(1+2\phi_1)+2\sigma_f(1-\phi_1)\sigma_{s_1}(1-\phi_1)+\sigma_f(2+\phi_1)\right],\\ (\rho\beta_T)_{hnf}&=(1-\phi_2)\left[(1-\phi_1)(\rho\beta_T)_f+\phi_1(\rho\beta_T)_{s_1}\right]+\phi_2(\rho\beta_T)_{s_2},\\ (\rho\beta_C)_{hnf}&=(1-\phi_2)\left[(1-\phi_1)(\rho\beta_C)_f+\phi_1(\rho\beta_C)_{s_1}\right]+\phi_2(\rho\beta_C)_{s_2},\\ \left(\rho C_p\right)_{hnf}&=(1-\phi_2)\left[(1-\phi_1)\left(\rho C_p\right)_f+\phi_1\left(\rho C_p\right)_{s_1}\right]+\phi_2\left(\rho C_p\right)_{s_2},\\ k_{hnf}&=k_{bf}\left[\frac{k_{s_2}+2k_{bf}-2\phi_2(k_{bf}-k_{s_2})}{k_{s_2}+2k_{bf}+\phi_2(k_{bf}-k_{s_2})}\right], k_{bf}=k_f\left[\frac{k_{s_1}+2k_f-2\phi_1(k_f-k_{s_1})}{k_{s_1}+2k_f+\phi_1(k_f-k_{s_1})}\right],\\ D_{hnf}&=(1-\phi_1)(1-\phi_2)D_f\end{aligned} \tag{2.10}$$

where$\phi_1=0$ (exclusive of suspension of silver nanoparticles) represents titania/ H_2O and ethylene glycol (Casson) nanofluids and $\phi_2=0$ (exclusive of suspension of TiO_2 nanoparticles) represents TiO_2/H_2O and ethylene glycol (Casson) nanofluid. Both $\phi_1=0=\phi_2$ correspond to the base fluid (H_2O and ethylene glycol). The thermo physical properties of water and ethylene glycol and solid nanoparticles (Agand TiO_2)

Let $q=u+iv$, we obtain that

$$\begin{aligned}\frac{\partial q}{\partial t}+2i\Omega q &= v_{hnf}\left(1+\frac{1}{\beta}\right)\frac{\partial^2 q}{\partial z^2}-\frac{\sigma B_0^2(\alpha_1+i\alpha_2)}{\rho_{hnf}}q-\frac{v_{hnf}}{K^*}\left(1+\frac{1}{\beta}\right)q\\ &\quad +g(\beta_T)_{hnf}(T-T_\infty)+g(\beta_C)_{hnf}(C-C_\infty)\end{aligned} \tag{2.11}$$

The non-dimensional variables are introduced as

$$u*=\frac{u}{u_0}, v*=\frac{v}{u_0}, z*=\frac{z}{\sqrt{v_f t_0}}, t*=\frac{t}{t_0}, \theta=\frac{T-T_\infty}{T_w-T_\infty}, \phi=\frac{C-C_\infty}{C_w-C_\infty}, M^2=\frac{\sigma_f B_0^2 v_f}{\rho_f u_0^2}$$

$$R^2 = \frac{\Omega v_f}{u_0^2}, K = \frac{K^* u_0^2}{v_f^2}, \mathrm{Gr} = \frac{g(\beta_T)_f v_f (T_w - T_\infty)}{u_0^3}, \mathrm{Gc} = \frac{g(\beta_C)_f v_f (C_w - C_\infty)}{u_0^3}$$

$$\mathrm{Pr} = \frac{(\mu C_p)_f}{k_f}, Q = \frac{Q_0 v_f}{(\rho C_p)_f u_0^2}, \mathrm{Sc} = \frac{v_f}{D_f}, \mathrm{Kr} = \frac{\mathrm{Kr}^* v_f}{u_0^2}$$

Using dimensionless variables, the following governing equations are obtained.

$$J_1 \frac{\partial q}{\partial t} = J_2 \left(1 + \frac{1}{\beta}\right) \frac{\partial^2 q}{\partial z^2} - \left(J_3 M^2 (\alpha_1 + i\alpha_2) + 2iR^2 + \frac{J_2}{K}\left(1 + \frac{1}{\beta}\right)\right) q + J_4 \mathrm{Gr}\theta + J_5 \mathrm{Gc}\phi$$

$$J_6 \frac{\partial \theta}{\partial t} = \frac{J_7}{\mathrm{Pr}} \frac{\partial^2 \theta}{\partial z^2} - Q\theta \qquad (2.12)$$

$$\frac{\partial \phi}{\partial t} = \frac{J_8}{\mathrm{Sc}} \frac{\partial^2 \phi}{\partial z^2} - \mathrm{Kr}\phi$$

The relevant non-dimensional initial and boundary conditions are as follows:

$q = 0, \theta = 0, \phi = 0$ for all $z > 0$ and $t \le 0$,

$q = e^t + \lambda \left(1 + \frac{1}{\beta}\right) \frac{\partial q}{\partial z}, \theta = \begin{cases} t & \text{if } 0 < \tau \le 1 \\ 1 & \text{if } \tau > 1 \end{cases}, \phi = t$ at $z = 0$, (2.13)

$q \to 0, \theta \to 0, \phi \to 0$ as $z \to \infty$ for $t > 0$

where $\lambda = \frac{\lambda_0 u_0}{v_f}$ is the slip parameter.

To solve the Equations using the Laplace transform technique with respect to the initial and boundary conditions the transformed equations

$$a_1 \frac{d^2 \bar{q}}{dz^2} - (s + \lambda_1)\bar{q} = -a_2 \bar{\theta} - a_3 \bar{\phi}$$

$$\frac{d^2 \bar{\theta}}{dz^2} - (s + a_5) a_4 \bar{\theta} = 0 \qquad (2.14)$$

$$\frac{d^2 \bar{\phi}}{dz^2} - (s + \mathrm{Kr}) a_{10} \bar{\phi} = 0$$

The boundary conditions in terms of transformed variables are as

$$\bar{q} = \frac{1}{s-1} + \lambda \left(1 + \frac{1}{\beta}\right) \frac{d\bar{q}}{dz}, \bar{\theta} = \frac{1}{s^2}(1 - e^{-s}), \bar{\phi} = \frac{1}{s^2} \text{ at } z = 0$$

$$\bar{q} \to 0, \bar{\theta} \to 0, \bar{\phi} \to 0 \text{ as } z \to \infty$$

Solving differential Equations (29)-(31) with the boundary conditions (32)-(33), we acquire the transformed solutions for velocity, temperature and concentrations $\bar{q}(z,s)$, $\bar{\theta}(z,s)$ and $\bar{\phi}(z,s)$ as

$$\bar{q}(z,s) = \left\{ \left(1 + \lambda b_5 \left(1 + \frac{1}{\beta}\right)\right)^{-1} \left[\frac{1}{s-1} + b_3 + b_4 + \lambda \left(1 + \frac{1}{\beta}\right)(b_1 + b_2)\right] \right\} e^{-b_5 z}$$

$$- b_3 e^{-b_1 z} - b_4 e^{-b_2 z}$$

$$\bar{\theta}(z,s) = \frac{1}{s^2}(1 - e^{-s}) e^{-\sqrt{(s+a_5)a_4}\, z} \qquad (2.16)$$

$$\bar{\phi}(z,s) = \frac{1}{s^2} e^{-\sqrt{(s+\mathrm{Kr})a_{10}}\, z}$$

Taking the inverse Laplace transforms for Equations (34)-(36), we acquire the solutions for the velocity distribution, temperature and concentration distributions after moving on the t-direction for the flow near a vertical surface with the ramped plate temperature specified as

$$q(z,t) = q_1(z,t) - H(t-1) q_1(z, t-1)$$

$$\theta(z,t) = f_1(\alpha_2, a_5, t) - H(t-1) f_1(\alpha_3, a_5, t-1) \qquad (2.17)$$

$$\phi(z,t) = f_1(\alpha_3, \mathrm{Kr}, t)$$

To emphasize the consequence of the ramped wall temperature on the flow field, this may be consequential to contrast such a nanofluid flow due to the uniform wall temperature. the condition $\theta(0,t) = 1$, for $t = 0$. Under the assumptions portrayed in this present paper, it is revealed that the

Industrial Engineering Journal
ISSN: 0970-2555
Volume : 53, Issue 6, No.4, June : 2024

temperature distribution and velocity fields for the flow over a surface by the uniform wall temperature may be articulated as follows.

$$q(z,t) = q_2(z,t)$$
$$\theta(z,t) = f_7(\alpha_1, a_5, 0, t) \quad (2.18)$$

The Nusselt number in terms of rate of heat transport near the plate surface $(z = 0)$ for the ramped wall temperature and the uniform wall temperature is derived from and is given by

$$\theta'(0,t) = -\left(\frac{\partial\theta}{\partial z}\right)_{z=0} = -\sqrt{a_4}\left(g_1(a_5,t) - H(t-1)g_1(a_5,t-1)\right)$$
$$\theta'(0,t) = -\left(\frac{\partial\theta}{\partial z}\right)_{z=0} = -\sqrt{a_4}g_7(a_5,0,t)$$

Discussion of the Numerical results

The exact solutions of the governing equations of the flow domain are obtained using the Laplace transform method. The flow is presided over by the nondimensional parameters, namely, Hartmann numberM, permeability parameter K, rotation parameter R, Casson Grashof number Gm, Hall parameter βe, ion slip parameter βi, φ1 and φ2 volume fractions of Ag and TiO2 respectively.

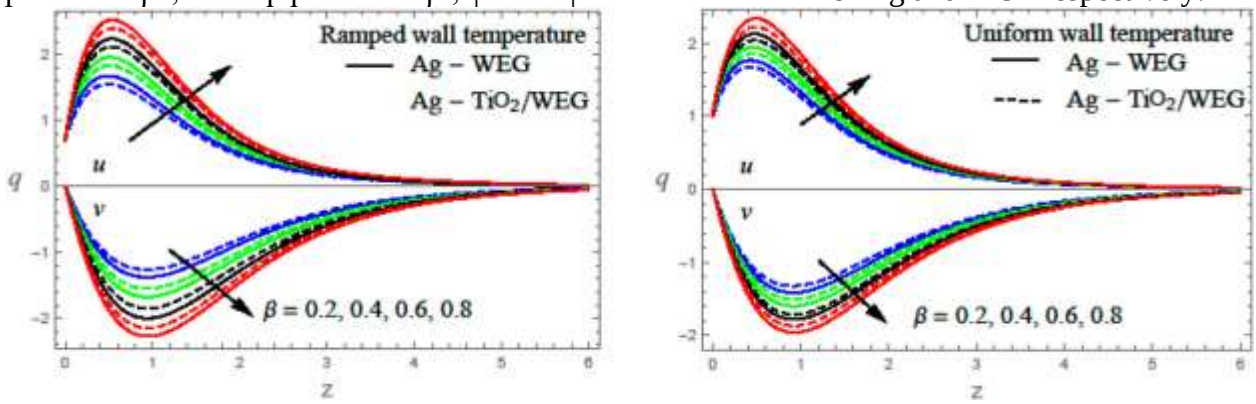

Figure.1 The velocity profiles against β.

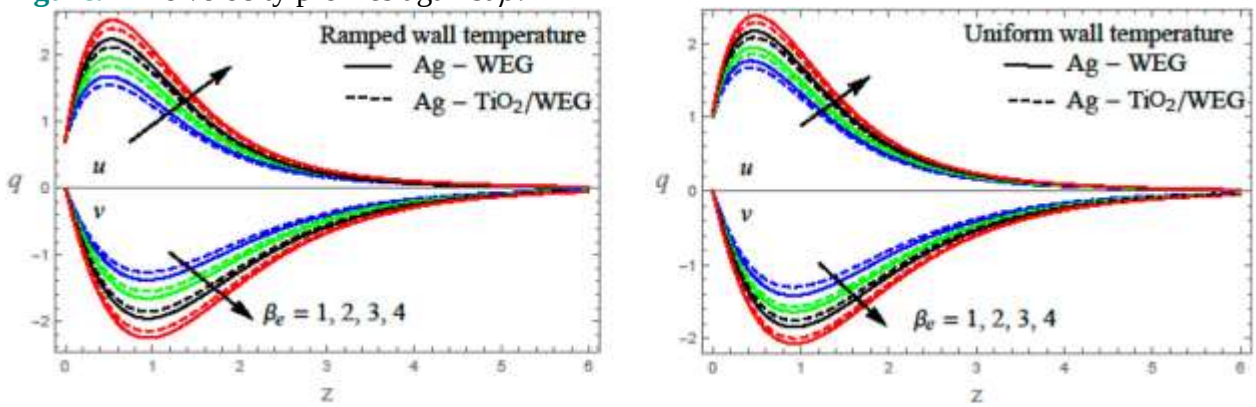

Figure .2 The velocity profiles against βe.

Industrial Engineering Journal
ISSN: 0970-2555
Volume : 53, Issue 6, No.4, June : 2024

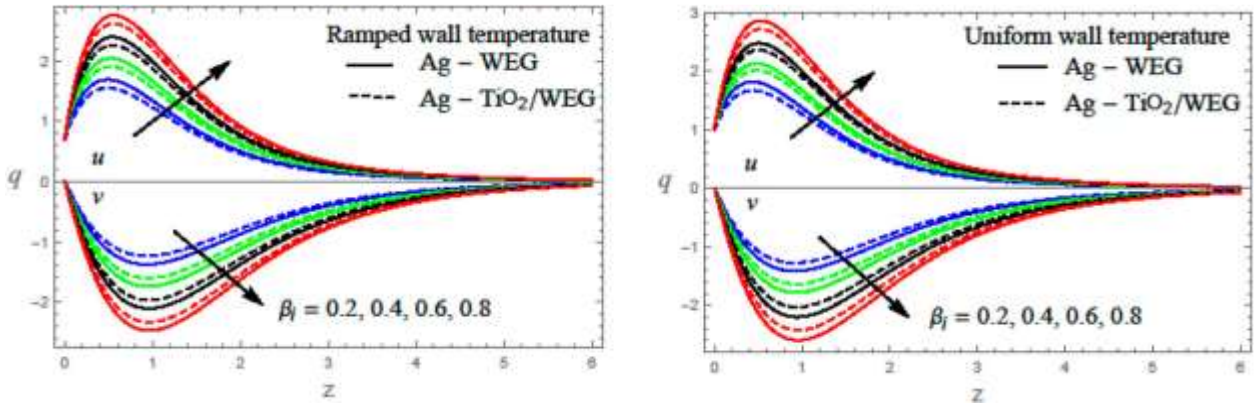

Figure.3 The velocity profiles against βi.

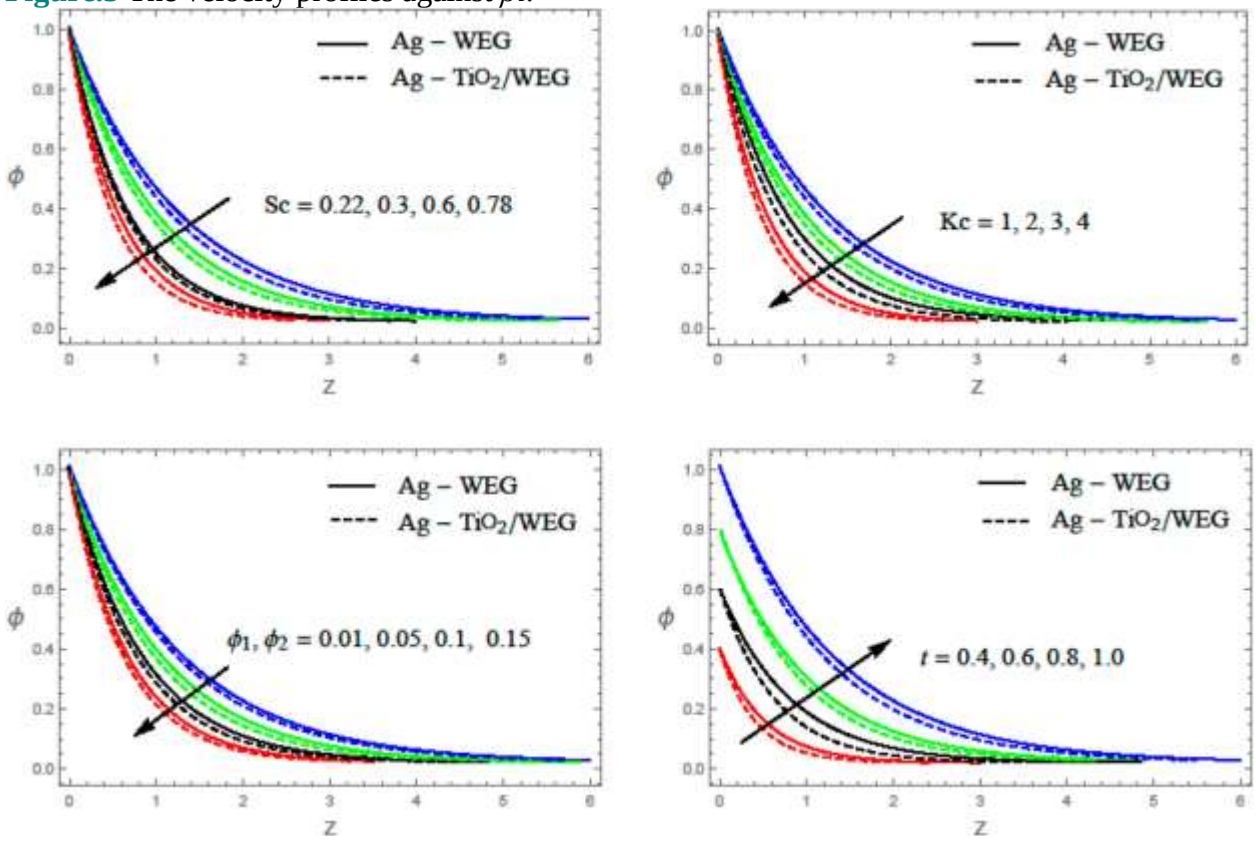

Figure. 4 The concentration profiles against Sc, Kc, $\varphi 1$, $\varphi 2$ and t.

It is apparent from Figure.1, the primary and secondary velocity components u and v of nanofluids Ag-WEG and Ag-TiO2/WEG for the ramped wall temperature and uniform wall temperature enlarge in the Casson fluid parameter. Consequently, the thickness of the boundary layer enlarges.

Figure.2 and 3 show that, for the nanofluids Ag-WEG and Ag-TiO2/WEG and the ramped wall temperature and uniform wall temperature, the primary velocity component u increases on an increase in Hall and ion slip parameters βe and βi, while the magnitude of second velocity component v augments on an increase in Hall and ion slip parameters throughout the fluid medium. It was obvious that strengthening in the Hall parameter and ion slip parameter enhanced the resulting velocity and the momentum boundary layer thickness throughout the fluid medium. The inclusion of Hall parameters reduces the effective conductivity and consequently moves down the magnetic renitent ferocity. In addition,the proficient conductance increases the ion slip parameter. For that motive, the attenuation forces decrease; as a result, velocity intensifies.

Figure.4 displays the influence of Schmidt number Sc, chemical reaction parameter Kc,and the volume fractions parameters φ1 and φ2 and time t on concentration profiles for nanofluids Ag-WEG and Ag-TiO2/WEG. The concentration distribution and boundary layer thickness are lessened with an increase in Sc. The Schmidt number is linearly relative to the ratio of the momentum diffusion to the mass diffusivity. Schmidt number hence measures a relative efficiency of momentum and mass transport through distribution into the hydrodynamic boundary layers. The reduction in the concentration profiles is accompanied by an instantaneous decrease in the concentration boundary layer thickness. The concentration profiles are reduced for escalating in chemical reaction parameter Kc. The larger values of Kc lead to reduce diffusion coefficient of hybrid chemical species. This declined concentration and boundary layer thickness. For a harmful case (Kc > 0), a constant chemical reaction faces lots of disturbance. These caused a large molecular movement in the operational hybrid nanofluid; this increased the transportation phenomenon, thus reducing the concentration distribution in the flow regimes. The persuasions of the volume fractions φ1 and φ2 of nanoparticles on concentration fields are evident that the concentration field and those comparative boundary layer thickness witness an increase in volume fractions φ1 and φ2. It may also be scrutinized that the nanoparticle concentrations are enhanced by an increment in time. Hence, it is noticed that the nanoparticle concentration is comparatively lesser in a hybrid nanofluid (Ag-TiO2/WEG) compared to a nanofluid (Ag-WEG).

References

[1] S. Choi, Enhancing thermal conductivity of fluids with nanoparticles, in: D.A. Siginer, H.P. Wang (Eds.), in: Developments and Applications of Non-Newtonian Flows, FED-Vol. 231, MD-Vol. 66, ASME, 1995, pp. 99–105.
[2] H. Masuda, A. Ebata, K. Teramae, N. Hishinuma, Alteration of thermal conductivity and viscosity of liquid by dispersing ultra-fine particles, NetsuBussei (Japan) 7 (4) (1993) 227–233.
[3] J. Buongiorno, Convective transport in nanofluids, ASME J. Heat Transfer 128 (2006) 240–250.
[4] S.K. Das, S. Choi, W. Yu, T. Pradeep, Nanofluids: Science and Technology, Wiley Interscience, New Jersey, 2007.
[5] J. Eastman, S.U.S. Choi, S. Lib, W. Yu, L.J. Thompson, Anomalously increased effective thermal conductivities of ethylene-glycol-based nanofluids containing copper nanoparticles, Appl. Phys. Lett. 78 (6) (2001) 718–720.
[6] J. Buongiorno, W. Hu, Nanofluid coolants for advanced nuclear power plants, in: paper no. 5705, Proc. ICAPP ’05, Seoul, May 15–19, 2005.
[7] A. Bejan, K.R. Khair, Heat and mass transfer by natural convection in a porous medium, Int. J. Heat Mass Transfer 28 (1985) 909–918.
[8] F.C. Lai, F.A. Kulacki, Coupled heat and mass transfer by natural convection from vertical surface in porous medium, Int. J. Heat Mass Transfer 34 (1991) 1189–1194.
[9] P.V.S.N. Murthy, P. Singh, Heat and mass transfer by natural convection in a non-Darcian porous medium, Acta Mech. 138 (1999) 243–254.
[10] F.C. Lai, Coupled heat and mass transfer by mixed convection from a vertical plate in a saturated porous medium, Int. Commun. Heat Mass Transfer 18 (1991) 93–106.
[11] O. Anwar Bég, H.S. Takhar, T.A. Bég, R. Bhargava, S. Rawat, Nonlinear Magneto-heat transfer in a fluid-particle suspension flowing via a non-Darcian channel with heat source and buoyancy effects: numerical study, J. Engrg. Sci. 19 (1) (2008) 63–88. King Abdul Aziz University.
[12] R. Bhargava, R. Sharma, O.A. Bég, Oscillatory chemically-reacting MHD free convection heat and mass transfer in a porous medium with Soret and Dufour effects: finite element modeling, Int. J. Appl. Math. Mech. 5 (6) (2009) 15–37.
[13] P. Cheng, Combined free and forced convection flow about inclined surfaces in porous media, Int. J. Heat Mass Transfer 20 (1977) 807–814.

[14] Ali J. Chamkha, Camille Issa, Khalil Khanafer, Natural convection from an inclined plate embedded in a variable porosity porous medium due to solar radiation, Int. J. Therm. Sci. 41 (2002) 73–81.
[15] Jamshed W, Aziz A. A comparative entropy based analysis of Cu and Fe3O4/methanol Powell-Eyering nanofluid in solar thermal collectors subjected to thermal radiation, variable thermal conductivity and impact of different nanoparticles shape. Results Phys. 2018;9: 195–205.
[16] Ellahi R. Special issue on recent developments of nanofluids. Appl Sci. 2018;8:192.
[17] Aman S, Zokri SM, Ismail Z, et al. Effect of MHD and porosity on exact solutions and flow of a hybrid Casson-nanofluid. J Adv Res Fluid Mech Therm Sci. 2018;44:131–139.
[18] Usman M, Hamid M, Zubair T, et al. Cu-Al2O3/water hybrid nanofluid through a permeable surface in the presence of nonlinear radiation and variable thermal conductivity via LSM. Int J Heat Mass Transf. 2018;126:1347–1356.
[19] Seadawy AR, Cheemaa N. Applications of extended modified auxiliary equation mapping method for high-order dispersive extended nonlinear Schrödinger equation in nonlinear optics. Modern Phys Lett B. 2019;33(18):1950203. doi:10.1142/S0217984919502038.
[20] Rizvi STR, Seadawy AR, Ali I, et al. Chirp-free optical dromions for the presence of higher order spatio-temporal dispersions and absence of self-phase modulation in birefringent fibers. Modern Phys Lett B. 2020;34(35):2050399. doi:10.1142/S0217984920503996.
[21] Seadawy AR, Cheemaa N. Propagation of nonlinear complex waves for the coupled nonlinear Schrödinger Equations in two core optical fibers. Physica A. 2019;529:121330. doi:10.1016/j.physa.2019.121330.
[22] Seadawy AR, Kumar D, Hosseini K, et al. The system of equations for the ion sound and Langmuir waves and its new exact solutions. Results Phys. 2018;9:1631–1634. doi:10.1016/j.rinp.2018.04.064.
[23] Rizvi STR, Seadawy AR, Ashraf F, et al. Lump and interaction solutions of a geophysical Korteweg–De Vries equation. Results Phys. 2020;19:103661. doi:10.1016/j.rinp.2020.103 661.
[24] Krishna MV. Radiation-absorption, chemical reaction, Hall and ion slip impacts on magnetohydrodynamic free convective flow over semi-infinite moving absorbent surface. Chin J Chem Eng.2021;31:1–13. doi:10.1016/cjche.2020.12.026.
[25] Krishna MV. Hall and ion slip effects on radiative MHD rotating flow of Jeffreys fluid past an infinite vertical flat porous surface with ramped wall velocity and temperature. Int Commun Heat Mass Transfer. 2021;126:105399. doi:10.1016/j.icheatmasstransfer.2021.105399.